Effect of Relative Humidity on the Oxidative and Physical Stability of Encapsulated Milk Fat

N. Hardas, S. Danviriyakul, J.L. Foley, W.W. Nawar, and P. Chinachoti*

Department of Food Science, University of Massachusetts, Amherst, Massachusetts 01003

ABSTRACT: Milk fat was used in this work as a model to study the effects of humidity and physical properties on lipid oxidation. Although milk fat is considered a relatively stable fat because of its low content of unsaturated FA, it can oxidize significantly under certain conditions, as observed, for example, in the case of dairy-based powders. Humidity and physical properties have a profound influence on the oxidative stability of powders containing fat, and these factors affect the surface and encapsulated fractions of the fat differently. To examine these effects, encapsulated milk fat powders were stored under conditions of controlled relative humidity. Oxidation of the encapsulated fat as assessed by measurements of PV, losses of FA, and hexanal production increased with increasing relative humidity (RH). At higher RH, moisture penetrates into the hydrophilic wall, interacting with and plasticizing the components, thereby making them less effective as moisture and oxygen barriers. Total oxidation of the powders was strongly influenced by the extent of oxidation in the encapsulated fraction (>98% of total lipids) although the surface fat fraction was oxidized more rapidly. Better protection against oxidation was obtained when fats were encapsulated and stored at 14 and 44% RH than at 52% RH.

Paper no. J9905 in *JAOCS 79*, 151–158 (February 2002).

KEY WORDS: Encapsulation, oxidation, physical stability, relative humidity, spray drying.

Stability of lipids is often improved by encapsulation. Entrapment of lipids in a wall matrix that serves as an oxygen and moisture barrier can increase their stability (1–3). During processing and storage, the slowing or inhibition of deteriorative reactions in encapsulated powders, such as lipid oxidation and nonenzymatic browning, is dependent on the ability to control molecular diffusion through a protective wall matrix and maintain the structural integrity that keeps emulsified lipids within each powder particle.

Lipid oxidation rate can vary with the humidity conditions of a food (4). Depending on the system, lipid oxidation has been reported to be rapid in both extremely dry and extremely moist environments. Under conditions of low water activity (a_w), [in general, at a_w < monolayer value, i.e., <4–5% moisture or <0.2–0.3 a_w (5,6)], oxidation is high (7). It has been suggested that this can be due to (i) binding of water to hydroperoxides upon addition of water at a low a_w range, interfering with their decomposition, (ii) a higher catalytic activity of transition metals when there is less hydrated water, and (iii) some other physical phenomena (e.g., physical protection by encapsulation). As a_w is increased from zero, lipid oxidation rate has been reported to decrease to a minimum (at around the monolayer value) and then increase. The increase has been suggested to result from an increase in mobility of the system, allowing catalysts to diffuse to the oil–water interface, and also from swelling and exposure of more catalytic sites of the macromolecules (8). Further addition of water ($a_w > 0.8$) results in a decrease in rate *via* quenching of free radicals and singlet oxygen, as well as a dilution effect on the catalysts (6,8).

In a low-moisture food, reaction rates can be limited by diffusion, and this has been proposed to be related to a glass-transition phenomenon (9,10). Oxidation has been proposed to be a function of $T - T_g$ (where T is experimental temperature and T_g is the glass transition temperature) in a case when sugar crystallization and structural change (collapse) occur in such a way that encapsulated lipids become exposed to air on the surface (10). However, in a study on lipid oxidation of freeze-dried sucrose–linoleic acid emulsions, sugar crystallization first led to a destabilization of the oil–water interface, resulting in coalescence of the droplets and powder fusion (11). As a result, some surface fat was further encapsulated. In this case, the oxidation rate was found to decrease with increasing a_w in this higher a_w range ($a_w > 0.6$).

Oxidative stability of powders containing fat is influenced by the presence of surface fat and powder porosity. In microencapsulated powders, surface fat (also known as easily extractable fat) and encapsulated fat (8) are subject to different local environments; therefore, it is important to monitor the stability of each fraction separately. Lipid oxidation was found to be faster in surface than in encapsulated linoleic acid in freeze-dried emulsions (12). Changes in physical properties of powders stored under different conditions may affect reaction rate differently. Release of encapsulated compounds due to lactose crystallization at high relative humidity (13–15) may accelerate reaction rates. In contrast, repartitioning of the surface fat into the encapsulated fraction, in freeze-dried sucrose–linoleic acid emulsions, resulted in a lower rate of oxidation (12). A better understanding of the effect of storage humidity on the oxidative stability of powders would be useful in the control of powder quality during storage.

The purpose of this study was to investigate the effect of humidity and physical properties on milk fat oxidation in powders during storage. In this work, PV was used as an indication of the initial products formed during autoxidation. The extent of oxidation was measured by the loss of substrate (PUFA) and analysis of hexanal. UV light was used to accelerate lipid oxidation. Powder structure was examined by scanning electron microscopy (SEM). Oil droplet size of reconstituted emulsions was measured using a light-scattering technique.

MATERIALS AND METHODS

Preparation of milk fat powders. Milk fat powders were prepared as previously described (16). The final composition of

*To whom correspondence should be addressed.

E-mail: pavinee@foodsci.umass.edu

the milk fat powders was 40% anhydrous milk fat (Glassland Dairy Products, Greenwood, WI), 2% lecithin (ADM Lecithin, Decatur, IL), 7.5% sodium caseinate (New Zealand Dairy Products USA, Santa Rosa, CA), 49.6% dextrose equivalent (DE) 36 corn syrup solids (Roquette America, Keokuk, IA), and 0.9% potassium phosphate dibasic (Fisher Scientific, Fairlawn, NJ). Three separate batches of powders were prepared. Each batch was stored and tested in triplicate, with the exception of hexanal analysis, which was done in duplicate (see below). All data reported show error bars representing variation among batches.

Storage and sampling. The encapsulated milk fat powder was stored in petri dishes at a depth of 1 cm. These were placed in an incubator maintained at 25 ± 0.5°C. UV-exposed samples were stored under two UV lamps (254 nm; Spectronics Corp.,Westbury, NY) placed 25 cm above the powder surface. Control (CT) samples were stored in the same incubator above the lamps. The humidity of the air in the incubator was maintained by the use of saturated salt solutions or silica gel and monitored with two thermohygrometers (Omega Engineering Inc., Stamford, CT) with the use of remote sensors placed on the same shelves as the samples. Data from the sensors were retrieved from a data logger (Campbell Scientific Inc., Logan, UT). Relative humidities (RH) of 14.5 ± 0.15% were maintained with silica gel, 43.7 ± 2.6% with saturated potassium carbonate, and 51.6 ± 1.3% with saturated sodium chloride in 24 × 40 cm trays. Apparently, the incubator recycled some outside air, and so the actual RH obtained did not match exactly the values expected for silica gel and saturated sodium chloride and saturated potassium carbonate solutions. The RH values reported here are those measured from the circulating air above the samples rather than the reference equilibrium RH for the corresponding saturated salt solutions. Powders were stirred for 5 min every day to ensure even exposure to light and UV.

Triplicate samples were taken at 0, 1, 2, 5, 8, 11, 15, and 20 d of incubation. The initial moisture content of freshly prepared powders was 0.85 ± 0.08% (total weight basis). The samples took 24 h to reach asymptotic moisture levels of 1.3 ± 0.1, 3.2 ± 0.3, and 4.8 ± 0.3% at 14, 44, and 52% RH, respectively. Moisture contents at the end of 15 d were 1.8 ± 0.2, 3.5 ± 0.5, and 4.4 ± 0.5% for 14, 44, and 52% RH, respectively.

Moisture content. Duplicate samples of approximately 2 g of powder were placed in tared aluminum dishes and dried for 24–48 h at 50°C in a vacuum oven at 29 in. Hg (17). Moisture content was calculated by weight difference.

Fat extraction. Surface fat was extracted from 2.5 g of powder by addition of 15 mL of hexane and vortexing for 2 min at room temperature followed by decanting and drying under N_2 gas (about 2.5 h) (16). Encapsulated fat was extracted by dispersing the washed powder (0.5 g of powder washed with 4 mL of hexane) in distilled water and extracting the fat with a hexane/isopropanol (2:1 vol/vol) mixture. The solvent phase was then dried under gentle flow of N_2 gas (20 min) to yield the encapsulated fat fraction. Difficulty in extraction of the encapsulated fat was observed in the oxidized powders, especially UV-exposed samples. The amount of recoverable encapsulated fat from these samples decreased with time. Extraction efficiency for both fractions was typically 80–100% of the initial fat present in the powder.

PV. Lipid peroxides were measured according to the methods of Jiang *et al.* (18) and the International Dairy Federation Standards (19), as modified by Shantha and Decker (20) and Hardas *et al.* (16). Samples (0.01–0.08 g fat) were mixed in a disposable glass tube with 3 mL of chloroform/methanol (2:1, vol/vol). Equal volumes (25 µL) of ammonium thiocyanate and Fe^{2+} solutions (0.005 g/mL) were added, and the tubes were then vortexed. After 20 min of incubation at room temperature, absorbance was measured at 500 nm. Peroxide concentrations were determined from a standard curve.

FA analysis. The extracted fat samples were methylated according to Glass (21). Triheptadecanoin (Sigma Chemical Co., St. Louis, MO) was used as internal standard. The methyl esters were analyzed in a Varian 3700 gas chromatograph equipped with a 30 m × 0.2 mm i.d. Supelcowax 10 column (Supelco, Bellefonte, PA).

Analysis of hexanal. Hexanal content was monitored by static headspace GC (22). A 5890 gas chromatograph (Hewlett-Packard, Avondale, PA) equipped with a 19395A Headspace Analyzer (Hewlett-Packard), 3392A Integrator (Hewlett-Packard), and a capillary column (Ultra 1, 50 m × 0.2 mm × 0.33 µm; Hewlett-Packard) was used. The column was maintained at 65°C, and the injector and detector were maintained at 180 and 250°C, respectively. Helium was used as a carrier gas. Hexanal standards (5 mL), each containing 0–10 µmol of hexanal in doubly distilled water, were used to construct a standard curve. For each sample analysis, 1 g of milk powder was placed in a 20-mL vial. Five milliliters of doubly distilled water was added, and the vial was capped with a polytetrafluoroethylene cap. After loading into the headspace analyzer and incubating at 50°C for 20 min, 1 mL of the headspace gas was injected. Hexanal content was determined from the intensity of the corresponding hexanal peak and the predetermined standard curve. All analyses were performed in duplicate. The experimental error was within 5%.

Emulsion droplet size distribution analysis. Powder was reconstituted to 10% solids (0.5 g of powder in 4.5 mL of distilled water, 50°C) before measuring oil droplet size distribution with a laser light-scattering particle size analyzer (LA-900; Horiba Instruments Inc., Irvine, CA). Two measurements were carried out on each of duplicate samples to determine the mean emulsion droplet size. At the point of measurement, the emulsion was further diluted to less than 0.02% (w/w) to prevent multiple scattering effects. A refractive index ratio of 1.08 was used to calculate the mean oil droplet size. In some cases, dispersed aliquots were observed under a light microscope (Nikon Eclipse 400; Nikon Inc., Melville, NY).

SEM. Internal and surface morphologies of the powders were evaluated by SEM. For the surface morphology, a thin layer of powder particles was attached to the specimen stub by Mikrostik Ultrathin adhesive (TED Pella, Inc., Tustin, CA).

To observe the internal structure, cross sections of the embedded powder were prepared. About 10 mg of powder was dispersed in 2 mL of LR-White resin and incubated under UV light

(~365 nm) for 24 h to polymerize the resin. The block containing embedded powder was sectioned by an ultramicrotome (Porter Blum Ultra-Microtome MT-2; Ivan Sorvall, Inc., Norwalk, CT) to expose the cut surface and then mounted onto a specimen stub with the use of epoxy resin as a binder.

All prepared specimens were then coated with a 400-Å palladium gold layer with the case of an E5100 SEM coating unit (Quantum Technologies, Newhaven, East Sussex, United Kingdom). The images were viewed with a scanning electron microscope at 3.0 kV (JSM 5400; JEOL, Peabody, MA) and 2000× magnification. Five frames were taken for each sample.

Statistical analysis. Statistical analysis was performed using SAS statistical software (SAS Institute Inc., Cary, NC). The general linear methods (GLM) procedure followed by the Student's *t*-test (LSD) was used to establish significance at $\alpha = 0.05$.

Three replicate batches of powder were stored at 14 and 52% RH and tested at least in duplicate for encapsulated PV, encapsulated FA, and moisture content ($n = 6$). When variations were high (e.g., when there was a very small amount of extractable fat), analyses were done in triplicate ($n = 9$).

RESULTS AND DISCUSSION

The encapsulated fat amounted to 96.5 ± 1.0 g/100 g of initial fat; the surface fat amounted to 2.4 ± 0.3 g/100 g of initial fat. The total extractable fat (encapsulated + surface) was >98% of the initial fat content. A preliminary investigation was done on the effects of drying temperature and DE of the maltodextrin used on surface and encapsulated lipids (23). It was found that the encapsulation efficiency was dependent on DE, which influenced the drying dynamics, leading to scars on the powder surfaces. Microscopic cracks present on the surface can allow solvent extraction of some inner lipids. This could explain the presence of higher amounts of surface lipids in some cases. High encapsulation efficiency (~98% encapsulated fat) was attributed to the type of wall material (DE 36 corn syrup solids), small emulsion droplet size (~ 0.5 μm), and the emulsifying effect of lecithin, which maintained emulsion stability. A decrease in surface fat was probably caused by softening of the wall matrix, depending on the amount of water sorbed and leading to some closing of pores, such that less fat became accessible to the solvent (13).

Except for the control (no UV), the amount of recovered encapsulated fat for samples stored at 14 and 44% RH decreased over time (data not shown). This discrepancy between recovered and expected encapsulated fat was greatest when oxidation was accelerated with UV light. The observed decline in extractability could have been due to protein polymerization enhanced by light and humidity.

Surface fat of the CT samples decreased ($\alpha = 0.05$) during the first 24 h of incubation at 44 or 52% RH, from approximately 2.4 to 1.4% of initial fat (Fig. 1A). After the first day at 44% RH, surface fat remained relatively constant whereas at 52% RH it increased with time, exceeding the initial level after 11 d of storage. Throughout the storage period at 14% RH, the change in surface fat was minimal for both CT and

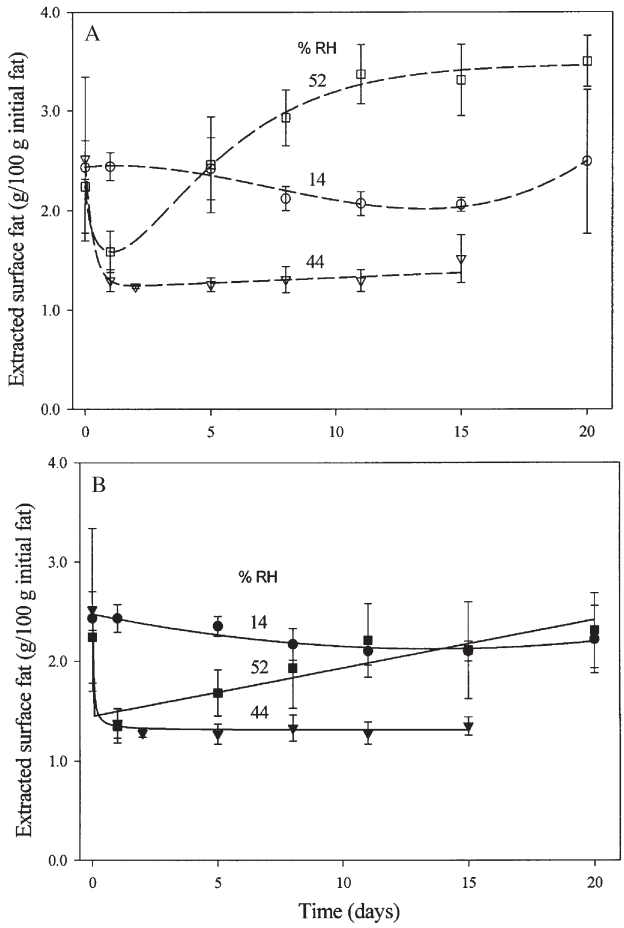

FIG. 1. Extracted surface fat (g/100 g initial fat) of (A) control powders stored at (○) 14 (▽), 44, and (□) 52% relative humidity (RH); and (B) UV-exposed powders stored at (●) 14, (▼) 44, and (■) 52% RH.

UV-exposed samples (Figs. 1A,B). Above a critical combination of temperature and humidity, increases in the surface fat of powders made with various sugars have been observed by several researchers (13,24,25). Decrease in surface fat could be caused by plasticization (softening) of wall material, leading to local viscous flow sealing off some pores or cracks (13). This may explain the early decrease in surface fat at 52% RH. The later increase in the amount of surface fat probably resulted from a phase transition (recrystallization), which was observed by DSC (23). It was reported earlier that crystallization could lead to an increase in surface fat in a freeze-dried emulsion system (26).

Oxidative stability. (i) PV. PV increased to a greater extent in surface fats ($\alpha = 0.05$) (Fig. 2A) than in the encapsulated fats (Fig 2B) for both UV-exposed and CT powders. UV light accelerated the oxidation process as measured by PV ($\alpha = 0.05$) in both surface and encapsulated fats. PV of the surface fat in the CT samples (Fig. 2A, dashed lines) was practically unchanged up to day 5. From day 8 to the end of the experiment, PV gradually increased ($\alpha = 0.05$). The highest increase was observed for the samples stored at 14% RH, followed by the samples stored at 44 and 52% RH, respectively. The PV of the encapsulated fat in the CT samples (Fig. 2B, dashed lines) remained relatively unchanged over 20 d of storage.

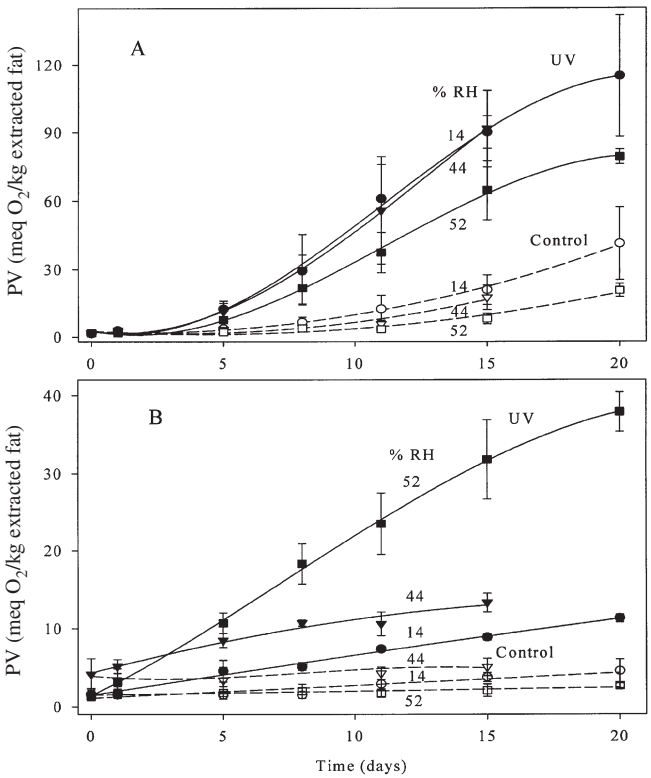

FIG. 2. Peroxide value (PV) meq O_2/kg extracted fat) of surface fat (A) and encapsulated fat (B) for control powders stored at (○) 14, (▽) 44, and (□) 52% RH and UV-exposed powders stored at (●) 14, (▼) 44, and (■) 52% RH. See Figure 1 for abbreviation.

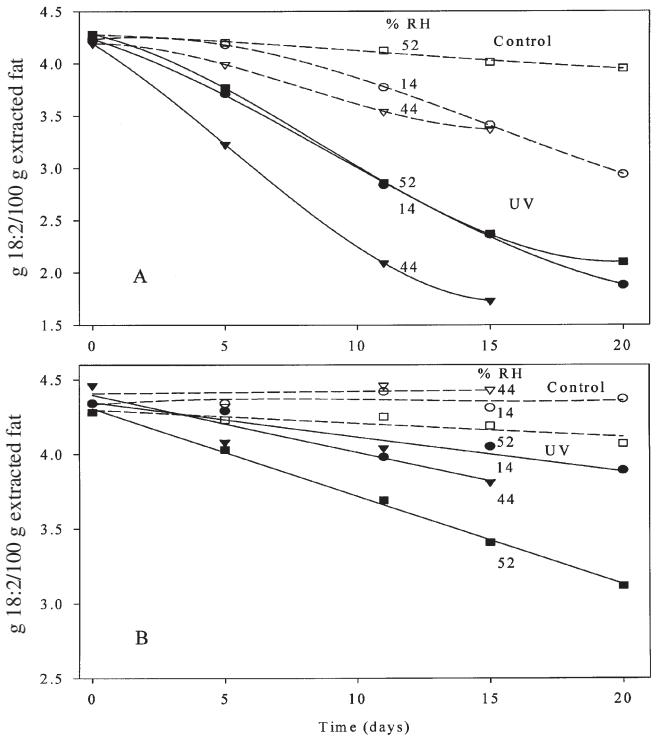

FIG. 3. Linoleic acid (18:2) content (g/100 g extracted fat) of surface fat (A) and encapsulated fat (B) for control powders stored at (○) 14, (▽) 44, and (□) 52% RH, and UV-exposed powders stored at (●) 14, (▼) 44, and (■) 52% RH. Standard deviations were within 0.03–0.50 g/100 g extracted fat. See Figure 1 for abbreviation.

The PV of UV-exposed samples increased significantly at all RH values for both surface (Fig. 2A, solid lines) and encapsulated (Fig. 2B, solid lines) fats. However, the increase was more pronounced in the case of the surface fat, showing higher oxidation rates at 14 and 44% RH than at 52% RH. In contrast, the encapsulated fat oxidized more rapidly at 52% RH than at 14 and 44% RH ($\alpha = 0.05$).

(ii) FA. Figures 3 and 4 show the changes during storage in linoleic (18:2) and linolenic (18:3) acid contents, respectively, of the surface and encapsulated fats. The initial values were 4.3 ± 0.3 and 0.61 ± 0.0 g/100 g of extracted fat for 18:2 and 18:3 fatty acids, respectively. The relatively high level of 18:2 FA was due to the incorporation of soy lecithin (5% of the total lipids). At all RH values, the 18:2 and 18:3 FA in the encapsulated fat of the CT samples (Figs. 3B and 4B) remained constant over the storage period. A decrease in the amounts of these FA was found in the encapsulated fat of the UV-exposed samples. This decrease was faster at 52% RH ($\alpha = 0.05$) than at 14 or 44% RH, in agreement with the PV data indicating that the encapsulated fat in the UV-exposed samples oxidized to the greatest extent at 52% RH.

The 18:2 and 18:3 FA in the surface fat of the CT samples decreased ($\alpha = 0.05$) when the samples were stored at 14 and 44% RH but remained relatively unaltered at 52% RH. The greatest decline in the 18:2 and 18:3 FA (Figs. 3A and 4A, solid lines) was observed for the surface fat of the UV-exposed samples at 44% RH, with slower rates of decline at 14

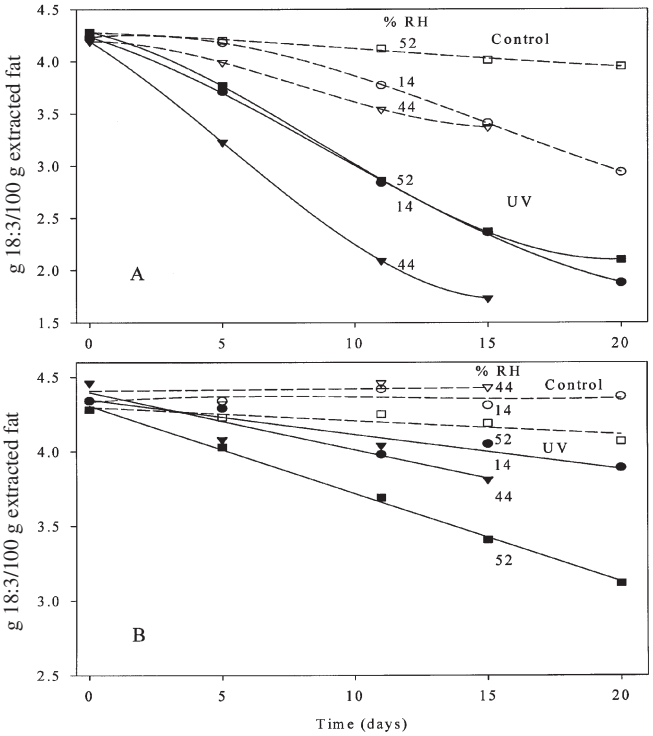

FIG. 4. Linolenic acid (18:3) content (g/100 g extracted fat) of surface fat (A) and encapsulated fat (B) for control powders stored at (○) 14, (▽) 44, and (□) 52% RH, and UV-exposed powders stored at (●) 14, (▼) 44, and (■) 52% RH. Standard deviations were within 0.01–0.10 g/100 g extracted fat. See Figure 1 for abbreviation.

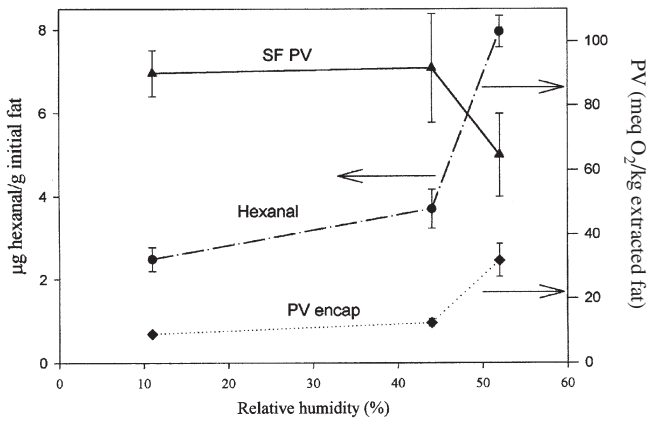

FIG. 5. Hexanal content (●, µg hexanal/g total fat in reconstituted emulsion) and PV (meq O_2/kg extracted fat) of encapsulated fat (◆) and surface fat (SF: ▲) of UV-exposed powders at 15 d. Initial hexanal content of day 0 powders was 0.09 ± 0.03 µg/g total fat. See Figure 2 for abbreviation.

and 52% RH. These results are consistent with the PV data obtained; i.e., the surface fat of the CT samples at 52% RH was the least oxidized of the surface fats.

(iii) Hexanal content. Figure 5 shows the effect of humidity on the accumulation of hexanal (measured at day 15) for the UV-exposed samples. These data are consistent with the PV data for the encapsulated fat (Fig. 2), as well as with the amount of 18:2 FA lost (data not shown). On the other hand, as RH increased from 44 to 52%, surface fat PV decreased while hexanal increased. The PV data indicate that the surface fat was oxidized to a higher extent than the encapsulated fat at all RH values. However, since the encapsulated fat amounted to >90% of the total extractable fat, its oxidation was the dominant factor in the accumulation of hexanal.

Powder morphology. The effect of humidity on the powder morphology is illustrated in Figures 6 and 7. Figure 6 shows the SEM micrographs of the powders after 15 d of storage

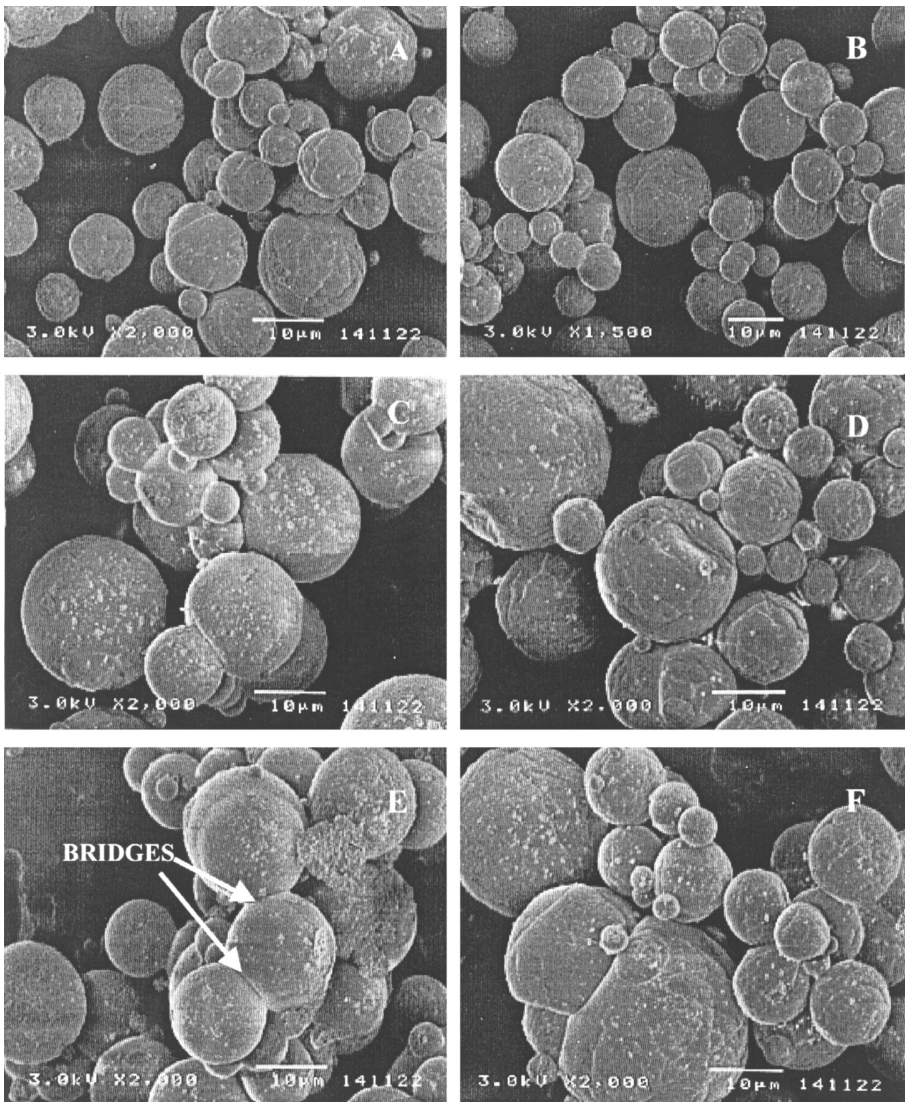

FIG. 6. Scanning electron micrographs illustrating the outer structure of spray-dried milk fat powders after 15 d of storage at 25°C under control and UV-exposed conditions at different humidities. (A) Control, 14% RH; (B) UV-exposed, 14% RH; (C) control, 44% RH; (D) UV-exposed, 44% RH; (E) control-52% RH; (F) UV-exposed, 52% RH. See Figure 1 for abbreviation.

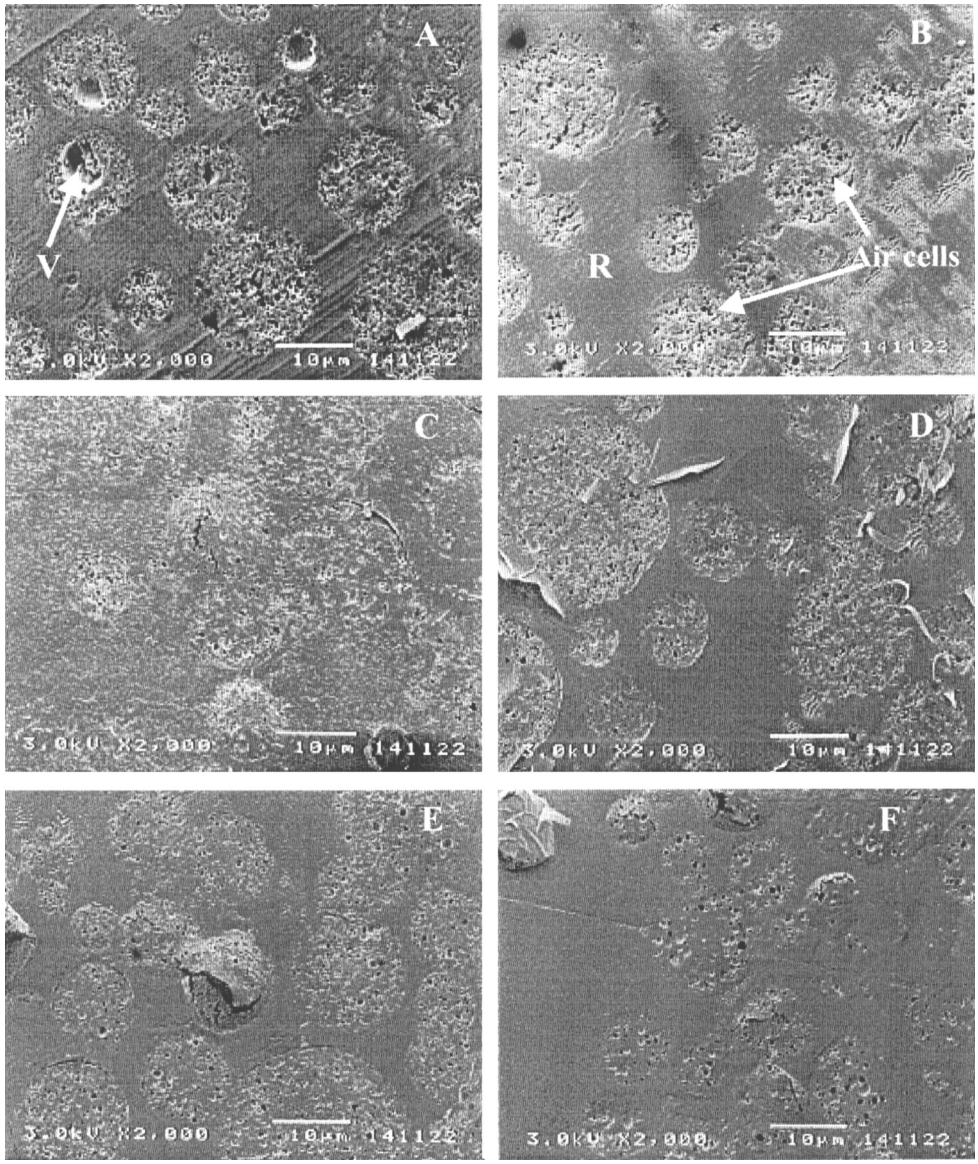

FIG. 7. Scanning electron micrographs illustrating the internal structure of spray-dried milk fat powders (embedded in resin) after 15 d of storage at 25°C under control and UV-exposed conditions at different humidities. (A) Control, 14% RH; (B) UV-exposed, 14% RH; (C) control, 44% RH; (D) UV-exposed, 44% RH; (E) control, 52% RH; (F) UV-exposed, 52% RH. V, void; R, embedded resins. See Figure 1 for abbreviation.

at 25°C under control and UV-exposed conditions. The powder particles were all spherical and 1–30 μm in diameter. As described in a previous study (16), powder surface and internal morphology can be evaluated by SEM. However, caution is necessary with respect to possible artifacts.

At 14 and 44% RH (Fig. 6A–D), there were no apparent changes in the structures of both CT and UV-exposed samples. At these humidities, the individual particles remained intact and did not clump together. At 52% RH, the particles started to stick or fuse and form interparticle bridges (indicated by arrows in Fig. 6). The bridge formation (observed when two round particles join on the surface, leading to a straight line in between, see arrows in Fig. 6) was more pronounced in the CT sample than in the UV-exposed sample. Additionally, the CT sample exhibited smoother surfaces with fewer wrinkles (Fig. 6E,F). These small differences between the CT and UV-exposed samples might be due to slight variation in the humidities inside the incubator, where the CT sample experienced a slightly higher humidity (2%) than the UV-exposed samples.

With regard to the powder internal structure, air cells were observed throughout the powder particles when stored at 14 and 44% RH (Fig. 7A–D). These SEM micrographs indicate that the powders were porous and contained air cells and large voids. The amount of air cells was less in the powders stored at 52% RH (Fig. 7E,F), and thus a denser internal structure was observed at this humidity as compared to the lower humidities (14 and 44% RH). Upon water sorption, the wall matrix of the powder became soft and more mobile owing to the plasticizing effect of water. This allowed the flow of semisolid materials, closing off the cracks. In extreme cases, this could lead to structural

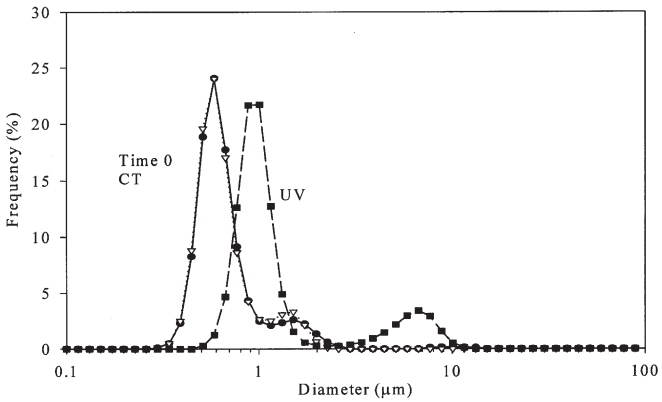

FIG. 8. Particle size distribution of reconstituted emulsions. Emulsions were made from the powder after spray-drying (time 0) (▽) and 20 d after storage under control (CT) (●) and UV-exposed (■) conditions at 52% RH and 25°C. The analyses were performed 30 min after reconstitution at 50°C in distilled water. See Figure 1 for abbreviation.

collapse (2,3,24,25). Like our previous study (23), the present work indicated that, with increase in humidity, DE 36 corn syrup solid was plasticized and the wall material softened and started to stick to other particles (observed at about 52% RH).

Embedding resins have been shown to affect the interpretation of the internal structure (16). For instance, when the internal structure is examined by observing a cut surface of embedded powders, embedding resins might leave artifacts on the fine-detail morphology. LR-white resin, which was used in the present study, performed better than epoxy resin (16). Further discussion of SEM applications to dairy products can be found elsewhere (27,28).

Emulsion oil droplet size distribution. The mean droplet diameter of the CT samples after reconstitution in distilled water (50°C) remained relatively constant (~0.5 μm) over the storage period. No difference in the distribution was observed in the CT samples at all relative humidities studied.

UV-exposed samples showed some decrease in their dispersibility with storage time, especially at higher RH (Figs. 8 and 9). After 5 d of storage at 44 and 52% RH, the reconstituted emulsions from these samples (in distilled water, 50°C) showed broader oil droplet size distributions than those of the original and CT samples (Fig. 8). A greater number of large particles (~5 μm) was observed as a result of clumping or flocculation of droplets (Fig. 8). The size distribution became narrower over time after reconstitution as the clumped particles dispersed, eventually reaching the same distribution as the emulsion of the CT or the initial sample. This indicates a reversible (loose) flocculation. Figure 9 shows a microscopic observation after reconstitution. Complete dispersion of the CT and UV-treated particles (44% RH) was obtained after 30 min of reconstitution in warm distilled water (50°C). At 52% RH, a longer suspension time was needed because some particles (only a small number) remained undispersed even after 1 h under the same conditions. This observation coincided with a decrease in encapsulated fat extractability of these powders. During fat extraction of these powders, a thicker interfacial layer between the organic and aqueous phases was observed. This indicated that the powders were not readily dissolved in water and formed an intermediate emulsion upon mixing with the extracting solvent as compared to freshly spray-dried, CT, or less oxidized samples. This observation suggests that cross-linking among lipids, lipid decomposition products, or lipids and proteins may have occurred *via* UV-induced reactions (including UV-induced oxidation). Owing to loss of protein functionality and the production of modified structures, it would then not be easy to disrupt the wall matrix when the powders were dispersed in water. Although the coalescence of oil droplets at higher RH (75%) in freeze-dried linoleic acid–sucrose emulsion was reported by Ponginebbi *et al.* (12), no coalescence was observed at any of the RHs studied in this work.

Water sorption isotherms of the sample showed a typical sigmoidal curve (23). The effect of sample a_w on the rates of oxidation of the surface lipid fraction and the encapsulated fraction were interestingly different. The encapsulated fraction exhibited a lower rate at lower a_w and the highest rate at the highest a_w (0.52), whereas the surface fraction exhibited the slowest oxidation at 0.52 a_w. This demonstrates the importance of the physical environment and the effect of surrounding materials on the oxidation of the lipids. In the case of the encapsulated lipids, the wall matrix protects the lipids from moisture

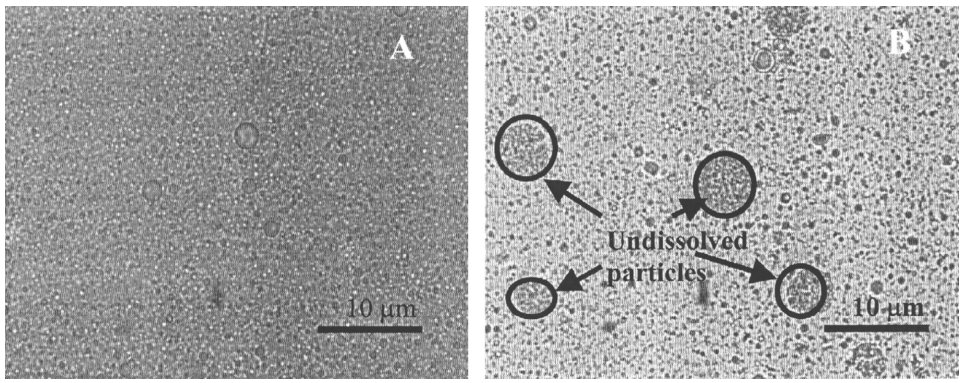

FIG. 9. Micrographs of reconstituted emulsions of powders after 20 days of storage at 52% RH and 25°C: (A) control; (B) UV-exposed samples. The pictures were taken 30 min after reconstitution at 50°C in distilled water. See Figure 1 for abbreviation.

and oxygen in the air; thus, the controlling factor is molecular diffusion through the wall matrix. Hydration leads to plasticization (glassy–rubbery transition), reducing the local viscosity and thereby allowing smaller molecules to diffuse through the matrix (29). Thus, oxidation was found to increase with increasing a_w. In the case of the surface lipids, which are directly exposed to air and humidity, oxidation is not limited by diffusion through the powder matrix. Drier storage air promotes oxidation of the surface lipids. The faster rate of oxidation at lower a_w could be related to less interference from water molecules, which hydrate the localized catalysts.

ACKNOWLEDGMENTS

Financial support was provided by Dairy Management, Inc., and by the Cooperative State Research Extension, Education Service, USDA, Massachusetts Agricultural Experimental Station under Project No. 811.

REFERENCES

1. Karel, M., M.P. Buera, and Y. Roos, Effects of Glass Transitions on Processing and Storage, in *The Glassy State in Foods*, edited by J.M.V. Blanshard and P.J. Lillford, Nottingham University Press, Loughborough, Leicestershire, 1992.
2. Karel, M., and J.M. Flink, Some Recent Developments in Food Dehydration Research, in *Advances in Drying,* edited by A.S. Mujumdar, Hemisphere Publishing, Washington, DC, 1983, pp. 103–154.
3. To, E.C., and J.M. Flink, "Collapse," a Structural Transition in Freeze Dried Carbohydrates. II. Effect of Solute Composition, *J. Food Technol. 13*:567 (1978).
4. Labuza, T.P., Kinetics of Lipid Oxidation in Foods, *CRC Crit. Rev. Technol. 2*:355–405 (1971).
5. Brunauer, S., P.H. Emmett, and E. Teller, Adsorption of Gases in Multimolecular Layers, *J. Am. Chem. Soc. 60*:309 (1938).
6. Fritsch, C.W., Lipid Oxidation—The Other Dimensions, *inform 5*:423 (1994).
7. Nelson, K.A., and T.P. Labuza, Relationship Between Water and Lipid Oxidation Rate—Water Activity and Glass Transition Theory, in *Lipid Oxidation in Food*, edited by A.J. St. Angelo, ACS Symposium Series No. 500, American Chemical Society, Washington, DC, 1992, pp. 93–103.
8. Karel, M., and S. Yong, Autoxidation-Initiated Reactions in Food, in *Water Activity: Influences on Food Quality*, edited by L.B. Rockland and G.F. Stewart, Academic Press, New York, 1981, pp. 511–529.
9. Simatos, D., and M. Karel, Characterization of Water in Foods: Physico-chemical Aspects, in *Preservation by Moisture Control*, edited by C.C. Seow, Elsevier Applied Science, London, pp. 1–41.
10. Roos, Y., and M. Karel, Plasticizing Effect of Water on Thermal Behavior and Crystallization of Amorphous Food Models, *J. Food Sci. 56*:266–267 (1991).
11. Ponginebbi, L., Influence of Physical Properties on Oxidation in Liquid and Freeze-Dried Linoleic Acid/Sucrose/Maltodextrin Model Systems, Doctoral Dissertation, University of Massachusetts (Amherst), 1999.
12. Ponginebbi, L., W.W. Nawar, and P. Chinachoti, Moisture Induced Structural Changes in Freeze-Dried Emulsions Affect Lipid Oxidation, *Grasas Aceites 51*:348–354 (2000).
13. Moreau, D., and M. Rosenberg, Microstructure and Fat Extractability in Microcapsules Based on Whey Proteins or Mixtures of Whey Proteins and Lactose, *Food Struct. 12*:457 (1993).
14. Shahidi, F., and X.-Q. Han, Encapsulation of Food Ingredients, *Crit. Rev. Food Sci. Nutr. 33*:501 (1993).
15. Flink, J., and F. Gejl-Hansen, Retention of Organic Volatiles in Freeze-Dried Carbohydrate Solutions: Microscopic Observations, *J. Agric. Food Chem. 20*:691 (1972).
16. Hardas, N., S. Danviriyakul, J.L. Foley, W.W. Nawar, and P. Chinachoti, Accelerated Studies of Microencapsulated Anhydrous Milk Fat, *Lebensm. Wiss. Technol. 33*:506 (2000).
17. *Official Methods of Analysis of the Association of Official Analytical Chemists*, Association of Official Analytical Chemists, Arlington, 1973, Method 925.09.
18. Jiang, Z.H., J.V. Hunt, and S.P. Wolff, Ferrous Ion Oxidation in the Presence of Xylenol Orange for Detection of Lipid Hydroperoxide in Low-Density Lipoprotein, *Anal. Biochem. 202*:384 (1992).
19. *International IDF Standards*, International Dairy Federation, Brussels, 1991, Section 74A:1991.
20. Shantha, N.C., and E.A. Decker, Rapid, Sensitive, Iron-Based Spectrophotometric Methods for Determination of Peroxide Values of Food Lipids, *J. AOAC Internat. 77*:421–424 (1994).
21. Glass, R.L., Alcoholysis, Saponification and the Preparation of Fatty Acid Methyl Esters, *Lipids 6*:919 (1971).
22. Frankel, E.N., and A.L. Tappel, Headspace Gas Chromatography of Volatile Lipid Perodixation Products from Human Red Blood Cell Membranes, *Lipids 26*:479 (1987).
23. Danviriyakul, S., The Properties of Spray-Dried Milk Fat Emulsions as Affected by Types of Wall Materials and Processing and Storage Conditions, Doctoral Dissertation, University of Massachusetts (Amherst), 2001.
24. Gejl-Hansen, F., and J.M. Flink, Freeze-Dried Carbohydrate-Containing Oil-in-Water Emulsions: Microstructure and Fat Distribution, *J. Food Sci. 42*:1049 (1977).
25. Minemoto, Y., S. Adachi, and R. Matsuno, Comparison of Oxidation of Methyl Linoleate Encapsulated with Gum Arabic by Hot-Air-Drying and Freeze-Drying, *J. Agric. Food Chem. 45*:4530 (1997).
26. Shimada, Y., Y. Roos, and M. Karel, Oxidation of Methyl Linoleate Encapsulated in Amorphous Lactose-Based Food Models, *Ibid. 39*:637 (1991).
27. Kalab, M., Scanning Electron Microscopy of Dairy Products: An Overview, *Scanning Electron Microsc. III*:261 (1979).
28. Kalab, M., Electron Microscopy of Milk Products: A Review of Techniques, *Ibid. III*:453 (1981).
29. Chinachoti, P., Water Migration and Food Storage Stability, in *Food Storage Stability*, edited by I.A. Taub and R.P. Singh, CRC Press, Boca Raton, 1998, pp. 245–267.

[Received February 26, 2001; accepted November 20, 2001]